Inorg. Chem. **2005**, *44*, 1413–1420

High-Nuclearity Iridium Carbonyl Clusters Containing Phenylgermyl Ligands: Synthesis, Structures, and Reactivity

Richard D. Adams,* Burjor Captain, and Jack L. Smith, Jr.

Department of Chemistry and Biochemistry and the USC Nanocenter, University of South Carolina, Columbia, South Carolina 29208

Received October 24, 2004

The reaction of $Ir_4(CO)_{12}$ with Ph_3GeH at 97 °C has yielded the new tetrairidium cluster complexes $Ir_4(CO)_7(GePh_3)(\mu\text{-}GePh_2)_2[\mu_3\text{-}\eta^3\text{-}GePh(C_6H_4)](\mu\text{-}H)_2$ (**10**) and $Ir_4(CO)_8(GePh_3)_2(\mu\text{-}GePh_2)_4$ (**11**). The structure of **10** consists of a tetrahedral Ir_4 cluster with seven terminal CO groups, two bridging $GePh_2$ ligands, an ortho-metallated bridging $\mu_3\text{-}\eta^3\text{-}GePh(C_6H_4)$ group, a terminal $GePh_3$ ligand, and two bridging hydrido ligands. Compound **11** consists of a planar butterfly arrangement of four iridium atoms with four bridging $GePh_2$ and two terminal $GePh_3$ ligands. The same reaction at 125 °C yielded the two new triiridium clusters $Ir_3(CO)_5(GePh_3)(\mu\text{-}GePh_2)_3(\mu_3\text{-}GePh)(\mu\text{-}H)$ (**12**) and $Ir_3(CO)_6(GePh_3)_3(\mu\text{-}GePh_2)_3$ (**13**). Compound **12** contains a triangular Ir_3 cluster with three bridging $GePh_2$, one triply bridging GePh, and one terminal $GePh_3$ ligand. The compound also contains a hydrido ligand that bridges one of the Ir–Ge bonds. Compound **13** contains a triangular Ir_3 cluster with three bridging $GePh_2$ and three terminal $GePh_3$ ligands. At 151 °C, an additional complex, $Ir_4H_4(CO)_4(\mu\text{-}GePh_2)_4(\mu_4\text{-}GePh)_2$ (**14**), was isolated. Compound **14** consists of an Ir_4 square with four bridging $GePh_2$, two quadruply bridging GePh groups, and four terminal hydrido ligands. Compound **12** reacts with CO at 125 °C to give the compound $Ir_3(CO)_6(\mu\text{-}GePh_2)_3(\mu_3\text{-}GePh)$ (**15**). Compound **15** is formed via the loss of the hydrido ligand and the terminal $GePh_3$ ligand and the addition of one carbonyl ligand to **12**. All compounds were fully characterized by IR, NMR, single-crystal X-ray diffraction analysis, and elemental analysis.

Introduction

Main group metals such as tin and germanium are frequently used as modifiers for transition metal catalysts in a variety of chemical processes.[1] For example, rhodium catalysts containing either tin or germanium have been used in the selective hydrogenation of α,β-unsaturated aldehydes to unsaturated alcohols.[2] Iridium−tin catalysts have also shown high selectivity for hydrogenation as well as dehydrogenation reactions.[3] These and other catalysts are of great interest because of their close relation to well-studied systems such as platinum−tin.[4]

In recent studies, we have shown that Ph_3SnH is a useful reagent for introduction of large numbers of phenyl−tin ligands into polynuclear transition metal carbonyl cluster complexes. For example, the reaction of $Ru_5(CO)_{12}(C_6H_6)(\mu_5\text{-}C)$ with Ph_3SnH at 68 °C yielded two compounds: $Ru_5(CO)_{11}(SnPh_3)(\mu_5\text{-}C)(\mu\text{-}H)$ (**1**) and $Ru_5(CO)_{10}(SnPh_3)_2(\mu_5\text{-}C)(\mu\text{-}H)_2$ (**2**) by the oxidative addition of one and two molecules of Ph_3SnH, respectively.[5a] The same reaction at

* Author to whom correspondence should be addressed. E-mail: Adams@mail.chem.sc.edu.

(1) (a) Hermans, S.; Raja, R.; Thomas, J. M.; Johnson, B. F. G.; Sankar, G.; Gleeson, D. *Angew. Chem., Int. Ed.* **2001**, *40*, 1211. (b) Hermans, S.; Johnson, B. F. G. *Chem. Commun.* **2000**, 1955. (c) Candy, J. P.; Ferretti, O. A.; Mabilon, G.; Bournonville, J. P.; El Mansour, A.; Basset, J. M.; Martino, G. *J. Catal.* **1988**, *112*, 201. (d) Candy, J. P.; Ferretti, O. A.; Bournonville, J. P.; Mabilon, G. *Chem. Commun.* **1985**, 1197. (e) Holt, M. S.; Wilson, W. L.; Nelson, J. H. *Chem. Rev.* **1989**, *89*, 11. (f) Bondar, Z.; Mallat, T.; Bakos, I.; Szabo, S.; Zsoldos, Z.; Schay, Z. *Appl. Catal. A* **1993**, *102*, 105.

(2) (a) Lafaye, G.; Micheaud-Especel, C.; Montassier, C.; Marecot, P. *Appl. Catal. A* **2002**, *230*, 19. (b) Coupé J. N.; Jordão E.; Fraga M. A.; Mendes M. J. *Appl. Catal. A* **2000**, *199*, 45.

(3) (a) Somerville, D. M.; Shapley, J. R. *Catal. Lett.* **1998**, *52*, 123. (b) Lázár, K.; Bussière, P.; Guénin, M.; Fréty, R. *Appl. Catal.* **1988**, *38*, 19.

(4) (a) Ohta, M.; Ikeda, Y.; Igarashi, A. *Appl. Catal. A* **2004**, *266*, 229. (b) Delbecq, F.; Sautet, P. *J. Catal.* **2003**, *220*, 115. (c) Furcht, A.; Tungler, A.; Szabo, S.; Sarkany, A. *Appl. Catal. A* **2002**, *226*, 155. (d) Mahmoud, S.; Hammoudeh, A.; Gharaibeg, S.; *J. Mol. Catal. A* **2002**, *178*, 161. (e) Dahlenburg, L.; Mertel, S. *J. Organomet. Chem.* **2002**, *630*, 221. (f) Armendariz, H.; Guzman, A.; Toledo, J. A. *Appl. Catal. A* **2001**, *211*, 69.

(5) (a) Adams, R. D.; Captain, B. C.; Fu, W.; Smith, M. D. *Inorg. Chem.* **2002**, *41*, 5593. (b) Adams, R. D.; Captain, B. C.; Fu, W.; Smith, M. D. *Inorg. Chem.* **2002**, *41*, 2302.

10.1021/ic0485108 CCC: $30.25
Published on Web 02/03/2005

125 °C yielded two higher-nuclearity clusters: $Ru_5(CO)_8(\mu\text{-}SnPh_2)_4(\mu_5\text{-}C)$ (**3**) and $Ru_5(CO)_7(SnPh_3)(\mu\text{-}SnPh_2)_4(\mu_5\text{-}C)(\mu\text{-}H)$ (**4**).[5a,b] The mechanism for the addition of the $SnPh_2$ groups most likely begins with the activation of the Sn−H bond by the cluster as observed for compounds **1** and **2**. This is then followed by the cleavage of a Sn−Ph bond and subsequent elimination of benzene.

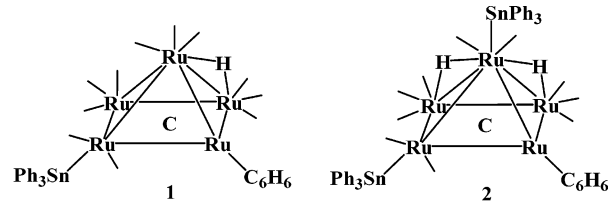

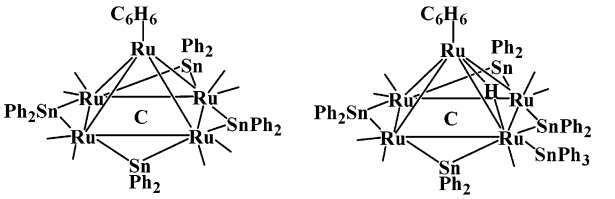

We have also found that Ph_3SnH reacts with the compounds $M_4(CO)_{12}$, M = Rh and Ir to yield the bimetallic cluster complexes $M_3(CO)_6(SnPh_3)_3(\mu\text{-}SnPh_2)_3$, M = Rh, **5**; M = Ir, **6**, containing an unprecedented number of phenyl−tin ligands.[6] Both compounds consist of triangular M_3 clusters with three bridging $SnPh_2$ and three terminal $SnPh_3$ ligands. Surprisingly, compound **5** reacts even further with Ph_3SnH at 151 °C to yield the compound $Rh_3(CO)_3(SnPh_3)_3(\mu\text{-}SnPh_2)_3(\mu_3\text{-}SnPh)_2$ (**7**), which contains eight phenyl−tin ligands.

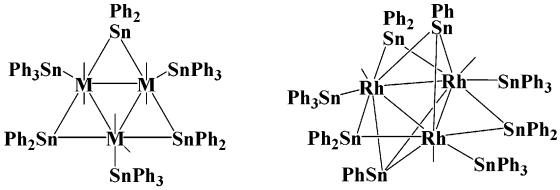

5: M = Rh
6: M = Ir
7

We have also shown that Ph_3GeH can be a useful reagent for synthesizing high-nuclearity ruthenium−germanium clusters.[7] For example, the complex $Ru_5(CO)_{15}(\mu_5\text{-}C)$ reacted with Ph_3GeH at 151 °C to give the compounds $Ru_5(CO)_{12}(\mu\text{-}GePh_2)_3(\mu_5\text{-}C)$ (**8**) and $Ru_5(CO)_{11}(\mu\text{-}GePh_2)_4(\mu_5\text{-}C)$ (**9**). The multiple addition of $GePh_2$ groups is similar to that observed for the reactions of Ph_3SnH.

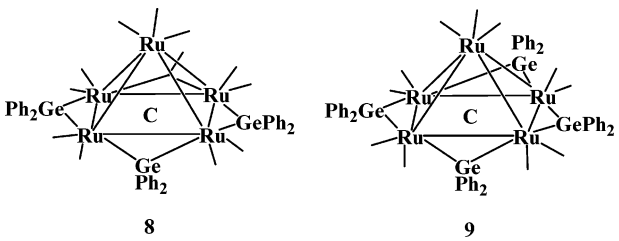

There are only a few examples of structurally characterized iridium−germanium complexes in the literature.[8] In this report, we describe our recent studies of the reactions of $Ir_4(CO)_{12}$ with Ph_3GeH at various temperatures. These studies have resulted in preparation of some the largest Ir−Ge cluster complexes reported to date. Five new compounds, including $Ir_4(CO)_7(GePh_3)(\mu\text{-}GePh_2)_2[\mu_3\text{-}\eta^3\text{-}GePh(C_6H_4)](\mu\text{-}H)_2$ (**10**), $Ir_4(CO)_8(GePh_3)_2(\mu\text{-}GePh_2)_4$ (**11**), $Ir_3(CO)_5(GePh_3)(\mu\text{-}GePh_2)_3(\mu_3\text{-}GePh)(\mu\text{-}H)$ (**12**), $Ir_3(CO)_6(GePh_3)_3(\mu\text{-}GePh_2)_3$ (**13**), and $Ir_4H_4(CO)_4(\mu\text{-}GePh_2)_4(\mu_4\text{-}GePh)_2$ (**14**), have been prepared and structurally characterized. We have also found that compound **12** reacts with CO at 125 °C to yield the new compound $Ir_3(CO)_6(\mu\text{-}GePh_2)_3(\mu_3\text{-}GePh)$ (**15**) by the addition of one carbonyl ligand and the loss of the bridging hydrido ligand and the one terminal $GePh_3$ ligand.

Experimental Section

General Data. All reactions were performed under a nitrogen atmosphere. Reagent grade solvents were dried by the standard procedures and were freshly distilled prior to use. Infrared spectra were recorded on a Thermo-Nicolet Avatar 360 FT-IR spectrophotometer. ^{1}H NMR spectra were recorded on a Mercury 300 spectrometer operating at 300.1 MHz. Elemental analyses were performed by Desert Analytics (Tucson, AZ). Product separations were performed by TLC in air on an Analtech 0.5 mm silica gel 60 Å F_{254} glass plates. $Ir_4(CO)_{12}$ was purchased from Strem Chemicals, Inc. Ph_3GeH was purchased from Aldrich and was used without further purification.

Reaction of $Ir_4(CO)_{12}$ with Ph_3GeH at 97 °C. Ph_3GeH (125 mg, 0.410 mmol) was added to a suspension of $Ir_4(CO)_{12}$ (30.0 mg, 0.0270 mmol) in 20 mL of heptane. The reaction mixture was heated to reflux for 8 h, after which the solvent was removed in vacuo. The product was separated by TLC using a 3:2 hexane/methylene chloride solvent mixture to yield 11.0 mg (21%) of yellow $Ir_4(CO)_7(GePh_3)(\mu\text{-}GePh_2)_2[\mu_3\text{-}\eta^3\text{-}GePh(C_6H_4)](\mu\text{-}H)_2$ (**10**) and 2.9 mg (4%) of red $Ir_4(CO)_8(GePh_3)_2(\mu\text{-}GePh_2)_4$ (**11**). Spectral data for **10**: IR ν_{CO} (cm^{-1} in hexane) 2082 (m), 2070 (s), 2043 (s), 2035 (m), 2024 (m), 1998 (m). ^{1}H NMR (CD_2Cl_2 in ppm at 25 °C) δ = 6.7−7.6 (m, 44 H, Ph), −17.63 (s, 1H, μ-H), −21.82 (s, 1H, μ-H). Calcd: 38.58 C, 2.63 H. Found: 38.40 C, 2.58 H. Spectral data for **11**: IR ν_{CO} (cm^{-1} in hexane) 2073 (w), 2045 (m), 2034 (m), 2027 (vs), 2008 (w). ^{1}H NMR (CD_2Cl_2 in ppm) δ = 6.8−7.5 (m, 70 H, Ph). Calcd (**11**·$^1/_2C_6H_6$): 44.80 C, 2.89 H. Found: 44.45 C, 2.80 H.

Conversion of 10 to 11. Ph_3GeH (20 mg, 0.066 mmol) was added to a solution of **10** (9.0 mg, 0.0046 mmol) in 10 mL of heptane. The reaction mixture was heated to reflux for 8 h, after which the solvent was removed in vacuo. The product was separated by TLC using a 3:2 hexane/methylene chloride solvent mixture to yield 4.0 mg (35%) of **11** as well as 2.5 mg (28%) of unreacted **10**.

Reaction of $Ir_4(CO)_{12}$ with Ph_3GeH at 125 °C. Ph_3GeH (125 mg, 0.41 mmol) was added to a suspension of $Ir_4(CO)_{12}$ (30 mg, 0.027

(6) Adams, R. D.; Captain, B. C.; Smith, J. L.; Hall, M. B.; Beddie, C. L.; Webster, C. E. *Inorg. Chem.* **2004**, *43*, 7576.
(7) Adams, R. D.; Captain, B. C.; Fu, W. *Inorg. Chem.* **2003**, *42*, 1328.
(8) (a) Feldman, J. D.; Peters, J. C.; Tilley, T. D. *Organometallics* **2002**, *21*, 4065. (b) Allen, J. M.; Brennessel, W. W.; Buss, C. E.; Ellis, J. E.; Minyaev, M. E.; Pink, M.; Warnock, G. F.; Winzenburg, M. L.; Young, V. G. *Inorg. Chem.* **2001**, *40*, 5279. (c) Hawkins, S. M.; Hitchcock, P. B.; Lappert, M. F.; Rai, A. K. *Chem. Commun.* **1986**, *23*, 1689. (d) Hawkins, S. M.; Hitchcock, P. B.; Lappert, M. F.; Rai, A. K. *Chem. Commun.* **1986**, 1689. (e) Bell, N. A.; Glockling, F.; Schneider, M. L.; Shearer, H. M.; Wilbey, M. D. *Acta Crystallogr., Sect. C* **1984**, *40*, 625.

Table 1. Crystallographic Data for Compounds **10**−**12**

compound	**10**	**11**	**12**
empirical formula	$Ir_4Ge_4O_7C_{61}H_{46}$	$Ir_4Ge_6O_8C_{92}H_{70}\cdot{}^1/_2C_6H_6$	$Ir_3Ge_5O_5C_{65}H_{51}\cdot{}^1/_2CH_2Cl_2$
formula weight	1950.14	2546.87	1894.07
crystal system	monoclinic	triclinic	monoclinic
lattice parameters			
a (Å)	10.4442(5)	11.6779(7)	12.8208(8)
b (Å)	23.0461(11)	12.3335(7)	21.4960(14)
c (Å)	24.1284(12)	17.2043(10)	23.5896(15)
α (deg)	90	76.525(1)	90
β (deg)	90.504(1)	89.661(1)	90.6010(10)
γ (deg)	90	71.842(1)	90
V (Å^3)	5807.4(5)	2283.7(2)	6500.8(7)
space group	*P*2(1)/c	$P\bar{1}$	*P*2(1)/c
Z	4	1	4
ρ_{calc} (g cm^{-3})	2.23	1.852	1.935
μ(Mo Kα) (mm^{-1})	11.219	7.798	8.481
temperature (K)	296	296	296
$2\Theta_{max}$ (deg)	52.04	50.06	50.06
no. of observations	9202	6585	9302
no. of parameters	693	525	705
goodness of fit	1.029	1.104	1.075
maximum shift in cycle	0.001	0.001	0.002
residuals [a]: R1; wR2 ($I > 2\sigma(I)$)	0.0307; 0.0667	0.0492; 0.1351	0.0347; 0.0961
absorption correction	SADABS	SADABS	SADABS
max/min	1.000/0.816	1.000/0.290	1.000/0.694
largest peak in final diff. map (e Å−3)	1.555	2.096	1.894

[a] $R = \sum_{hkl}(||F_{obs}| - |F_{calc}||)/\sum_{hkl}|F_{obs}|$; $R_w = [\sum_{hkl}w(|F_{obs}| - |F_{calc}|)^2/\sum_{hkl}wF^2_{obs}]^{1/2}$; $w = 1/\sigma^2(F_{obs})$; GOF $= [\sum_{hkl}w(|F_{obs}| - |F_{calc}|)^2/(n_{data} - n_{vari})]^{1/2}$.

mmol) in 20 mL of octane. The reaction mixture was heated to reflux for 5 h, after which the solvent was removed in vacuo. The product was separated by TLC using 3:2 hexane/methylene chloride solvent mixture to yield 8.5 mg (17%) of yellow $Ir_3(CO)_5(GePh_3)$-(μ-$GePh_2$)$_3$(μ_3-GePh)(μ-H) (**12**) and 2.2 mg (4%) of red $Ir_3(CO)_6$-$(GePh_3)_3$(μ-$GePh_2$)$_3$ (**13**). Spectral data for **12**: IR ν_{CO} (cm^{-1} in hexane) 2050 (s), 2029 (s), 2015 (m), 2000 (m), 1993 (m). ^{1}H NMR (CD_2Cl_2 in ppm) δ = 6.5−7.6 (m, 50 H, Ph), −14.17 (s, 1 H, μ-H). Calcd (**12**$\cdot{}^1/_2CH_2Cl_2$): 43.09 C, 2.99 H. Found: 42.94 C, 2.92 H. Spectral data for **13**: IR ν_{CO} (cm^{-1} in hexane) 2050 (m), 2010 (s). ^{1}H NMR (CD_2Cl_2 in ppm) δ = 6.7−7.4 (m, 75 H, Ph). Calcd (**13**$\cdot{}^1/_2CH_2Cl_2$): 49.96 C, 3.47 H. Found: 50.17 C, 3.82 H.

Conversion of 11 to 12. Ph_3GeH (18 mg, 0.059 mmol) was added to a solution of **11** (10 mg, 0.0040 mmol) in 10 mL of heptane. The reaction mixture was heated to reflux for 5 h, after which the solvent was removed in vacuo. The product was separated by TLC using a 3:2 hexane/methylene chloride solvent mixture to yield 3.0 mg (41%) of **12** as well as 2.5 mg (25%) of unreacted **11**.

Reaction of $Ir_4(CO)_{12}$ with Ph_3GeH at 151 °C. Ph_3GeH (125 mg, 0.41 mmol) was added to a suspension of $Ir_4(CO)_{12}$ (30 mg, 0.027 mmol) in 20 mL of nonane. The reaction mixture was heated to reflux for 2 h, after which the solvent was removed in vacuo. The product was separated by TLC using a 3:2 hexane/methylene chloride solvent mixture to yield 3.5 mg (7%) of **12**, 1.0 mg (2%) of **13**, and 14.2 mg (26%) of red $Ir_4H_4(CO)_4$(μ-$GePh_2$)$_4$(μ_4-GePh)$_2$ (**14**). Spectral data for **14**: IR ν_{CO} (cm^{-1} in hexane) 2025 (m), 2009 (s). ^{1}H NMR (CD_2Cl_2 in ppm) δ = 7.1−7.9 (m, 50 H, Ph), −12.21 (s, 4 H, Ir−H). Calcd (**13**$\cdot{}^1/_2CH_2Cl_2$): 36.75 C, 2.60 H. Found: 37.09 C, 2.56 H.

Conversion of 11 to 14. Hydrogen gas was bubbled through a suspension of **11** (10 mg, 0.0040 mmol) in 10 mL of nonane. The reaction mixture was heated to reflux for 2 h, after which the solvent was removed in vacuo. The product was separated by TLC using a 3:2 hexane/methylene chloride solvent mixture to yield 3.3 mg (39%) of **12**.

Reaction of 12 with CO. Compound **12** (10 mg, 0.0054 mmol) was dissolved in octane and heated to reflux under a slow purge of CO for 10 h. The solvent was then removed in vacuo, and the product was separated using a 3:2 hexane/methylene chloride solvent mixture to yield 7.9 mg (93%) of orange $Ir_3(CO)_6$(μ-$GePh_2$)$_3$(μ_3-GePh) (**15**). Spectral data for **15**: IR ν_{CO} (cm^{-1} in hexane) 2047 (w), 2021 (s), 2001 (s), 1989 (m). ^{1}H NMR (CD_2Cl_2 in ppm) δ = 6.7−7.7 (m, 35 H, Ph). Calcd: 36.61 C, 2.24 H. Found: 35.23 C, 2.24 H.

Crystallographic Analyses. Yellow crystals of **10** and **12**, red crystals of **13** and **14**, and orange crystals **15** were grown over a period of 1−2 days by slow evaporation of the solvent from a 3:1 hexane/CH_2Cl_2 solvent mixture at −18 °C. Red crystals of **11** were grown similarly from a 3:1 benzene/octane solvent mixture at 5 °C. Each data crystal was glued onto the end of a thin glass fiber. X-ray intensity data were measured by using a Bruker SMART APEX CCD-based diffractometer using Mo Kα radiation (λ = 0.71073 Å). The raw data frames were integrated with the SAINT+ program[9] by using a narrow-frame integration algorithm. Corrections for Lorentz and polarization effects were also applied with SAINT+. An empirical absorption correction based on the multiple measurement of equivalent reflections was applied using the program SADABS. All structures were solved by a combination of direct methods and difference Fourier syntheses and refined by full-matrix least-squares technique on F^2 using the SHELXTL software package.[10] All non-hydrogen atoms were refined with anisotropic displacement parameters unless otherwise noted. All phenyl hydrogen atoms were placed in geometrically idealized positions and included as standard riding atoms during the least-squares refinements. All hydrido ligands were located and refined with isotropic displacement parameters. Crystal data, data collection parameters, and results of the analyses are listed in Tables 1 and 2.

Compounds **10**, **12**, and **14** crystallized in the monoclinic crystal system. For these compounds, the space group $P2_1/c$ was identified uniquely on the basis of the systematic absences in the intensity data. One-half molecule of CH_2Cl_2 solvent was cocrystallized with both **12** and **14** and was located in each case and refined with isotropic displacement parameters and three geometric restraints.

(9) *SAINT+*, version 6.2a; Bruker Analytical X-ray Systems, Inc.: Madison, WI, 2001.
(10) Sheldrick, G. M. *SHELXTL*, version 6.1; Bruker Analytical X-ray Systems, Inc.: Madison, WI, 1997.

Table 2. Crystallographic Data for Compounds **13**−**15**

compound	**13**	**14**	**15**
empirical formula	$Ir_3Ge_6O_6C_{96}H_{75}\cdot{}^1/_2CH_2Cl_2$	$Ir_4Ge_6O_4C_{64}H_{54}\cdot{}^1/_2CH_2Cl_2$	$Ir_3Ge_4O_6C_{48}H_{35}$
formula weight	2379.16	2133.88	1574.72
crystal system	triclinic	monoclinic	triclinic
lattice parameters			
a (Å)	15.3856(5)	23.6617(10)	11.6076(7)
b (Å)	15.7158(5)	14.9749(6)	12.9334(8)
c (Å)	20.5575(6)	19.5807(8)	17.3520(11)
α (deg)	100.493(1)	90	98.003(1)
β (deg)	98.208(1)	103.784(1)	93.926(1)
γ (deg)	118.086(1)	90	114.303(1)
V (Å^3)	4159.8(2)	6738.2(5)	2328.1(2)
space group	$P\bar{1}$	*P*2(1)/c	$P\bar{1}$
Z	2	4	2
ρ_{calc} (g cm^{-3})	1.899	2.103	2.246
μ(Mo Kα) (mm^{-1})	7.001	10.582	11.133
temperature (K)	296	296	296
$2\Theta_{max}$ (deg)	50.06	50.06	56.04
no. of observations	11933	9936	8208
no. of parameters	1012	731	550
goodness of fit	1.021	1.045	1.018
maximum shift in cycle	0.001	0.002	0.001
residuals [a]: R1; wR2 ($I > 2\sigma(I)$)	0.0371; 0.0795	0.0296; 0.0749	0.0280; 0.0693
absorption correction	SADABS	SADABS	SADABS
max/min	1.000/0.774	1.000/0.451	1.000/0.449
largest peak in final diff. map (e Å−3)	1.504	1.407	1.864

[a] $R = \sum_{hkl}(||F_{obs}| - |F_{calc}||)/\sum_{hkl}|F_{obs}|$; $R_w = [\sum_{hkl}w(|F_{obs}| - |F_{calc}|)^2/\sum_{hkl}wF^2_{obs}]^{1/2}$; $w = 1/\sigma^2(F_{obs})$; GOF $= [\sum_{hkl}w(|F_{obs}| - |F_{calc}|)^2/(n_{data} - n_{vari})]^{1/2}$.

Compound **11** crystallized in the triclinic crystal system. The space group $P\bar{1}$ was assumed and confirmed by the successful solution and refinement of the structure. The metal atoms Ir(2) and Ge(1) were disordered equally over two sites and were refined with anisotropic displacement parameters. The carbonyl ligands C(21)−O(21) and C(22)−O(22), as well as the phenyl ring C(37)−C(42), were also found to be disordered over two positions, and they were each refined at 50% occupancy with isotropic displacement parameters. One-half molecule of benzene from the crystallization solvent cocrystallized with **11** and was located and refined with isotropic displacement parameters and 24 geometric restraints.

Compounds **13** and **15** also crystallized in the triclinic crystal system. For both compounds, the space group $P\bar{1}$ was assumed and confirmed by the successful solution and refinement of the structures. One-half molecule of CH_2Cl_2 solvent was cocrystallized with **13** and was located and refined with isotropic displacement parameters and three geometric restraints.

Results and Discussion

The reaction of $Ir_4(CO)_{12}$ with an excess of Ph_3GeH at 97 °C yielded two new tetrairidium cluster complexes $Ir_4(CO)_7(GePh_3)(\mu\text{-}GePh_2)_2[\mu_3\text{-}\eta^3\text{-}GePh(C_6H_4)](\mu\text{-}H)_2$ (**10**) and $Ir_4(CO)_8(GePh_3)_2(\mu\text{-}GePh_2)_4$ (**11**) in 21 and 4% yields, respectively. At 125 °C, the same reaction yielded two additional new triiridium clusters $Ir_3(CO)_5(GePh_3)(\mu\text{-}GePh_2)_3(\mu_3\text{-}GePh)(\mu\text{-}H)$ (**12**) and $Ir_3(CO)_6(GePh_3)_3(\mu\text{-}GePh_2)_3$ (**13**) in 17 and 4% yields, respectively, and at 151 °C, the reaction yielded still another new complex, a tetrairidium cluster $Ir_4H_4(CO)_4(\mu\text{-}GePh_2)_4(\mu_4\text{-}GePh)_2$ (**14**) in 26% yield. See Scheme 1. All five compounds were characterized by a combination of IR, ^{1}H NMR, single-crystal X-ray diffraction, and elemental analysis.

An ORTEP diagram of the molecular structure of **10** is shown in Figure 1. Selected intramolecular bond distances and angles are listed in Table 3. Compound **10** consists of an Ir_4 tetrahedron with two $GePh_2$ ligands and one μ_3-η^3-$GePh(C_6H_4)$ ligand formed by ortho-metallation of a phenyl ring bridging the Ir(1)−Ir(2)−Ir(3) triangle. This type of interaction has been observed for phosphido ligands, as found in the compounds $Ru_6(CO)_{14}(\mu\text{-}PMe_2)[\mu_3\text{-}\eta^2\text{-}PMe_2(C_6H_4)](\mu_6\text{-}C)$[11] and $Ir_7(CO)_{14}(\mu\text{-}PPh_2)[\mu_3\text{-}\eta^2\text{-}PPh(C_6H_4)]$,[12] but has not been observed previously for germanium-containing ligands. The complex also contains one $GePh_3$ ligand terminally coordinated to Ir(1). The ^{1}H NMR spectrum of **10** shows two resonances at −17.63 and −21.82 ppm, indicating the presence of two inequivalent hydrido ligands. Both hydrido ligands were located and refined crystallo-

Scheme 1

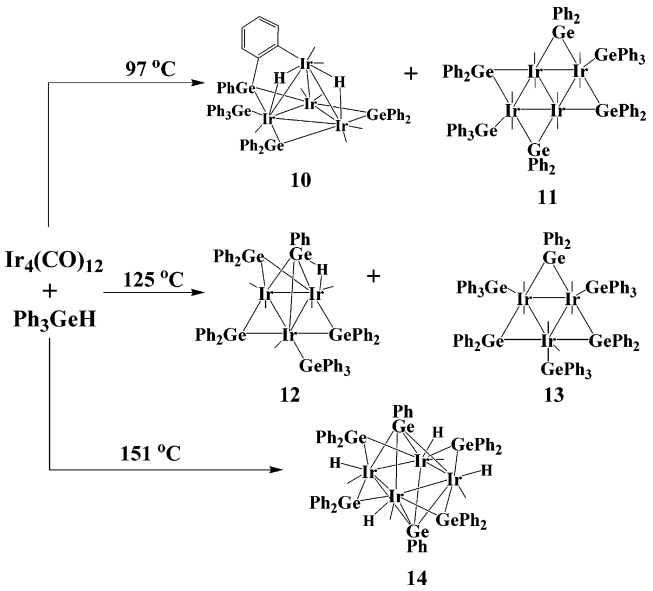

(11) Adams, R. D.; Captain, B.; Fu, W.; Smith, M. D. *J. Organomet. Chem.* **2002**, *651*, 124.
(12) de Araujo, M. H.; Vargas, M. D.; Braga, D.; Grepioni, F. *Polyhedron* **1998**, *17*, 2865.

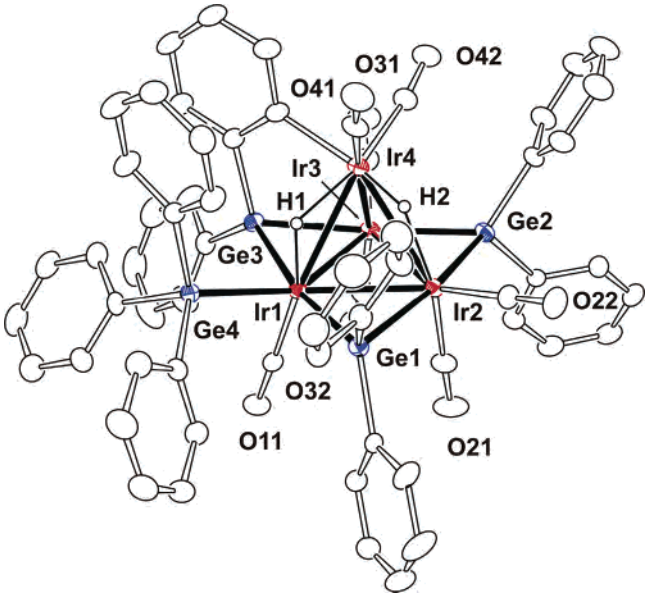

Figure 1. ORTEP diagram of the molecular structure of $Ir_4(CO)_7(\mu\text{-}H)_2(GePh_3)(\mu\text{-}GePh_2)_2(\mu\text{-}GePhC_6H_4)$ (**10**) showing 30% thermal ellipsoid probabilities.

Table 3. Selected Intramolecular Distances and Angles for Compounds **10** and **11**[a]

		10	
Ir(1)−Ir(2)	2.8340(4)	Ir(1)−Ge(3)	2.4474(7)
Ir(1)−Ir(3)	2.7983(4)	Ir(1)−Ge(4)	2.5201(7)
Ir(1)−Ir(4)	2.8895(4)	Ir(2)−Ge(1)	2.5660(7)
Ir(2)−Ir(3)	2.7672(4)	Ir(2)−Ge(2)	2.5036(7)
Ir(2)−Ir(4)	2.9744(4)	Ir(3)−Ge(2)	2.4838(8)
Ir(3)−Ir(4)	2.7230(4)	Ir(3)−Ge(3)	2.5117(8)
Ir(1)−Ge(1)	2.4518(7)	C−O (avg)	1.13(2)
Ge(1)−Ir(1)−Ge(4)	93.12(2)	Ge(2)−Ir(2)−Ir(3)	55.961(18)
Ge(1)−Ir(1)−Ir(4)	94.349(19)	Ge(3)−Ir(1)−Ge(1)	169.43(3)
Ge(1)−Ir(1)−Ir(3)	116.365(19)	Ge(4)−Ir(1)−Ir(3)	146.672(19)
		11	
Ir(1)−Ir(2A)	2.9070(10)	Ir(1)−Ge(3)	2.5246(11)
Ir(1)−Ir(2B)*	3.2277(11)	Ir(1)*−Ge(2)	2.5287(10)
Ir(1)*−Ir(2A)	3.0715(10)	Ir(1)*−Ge(1B)*	2.543(6)
Ir(1)*−Ir(2B)*	3.3720(11)	Ir(2A)−Ge(2)	2.6113(16)
Ir(2A)−Ir(2B)*	2.7690(10)	Ir(2B)*−Ge(1B)*	2.523(4)
Ir(1)−Ge(1A)	2.672(7)	Ir(2B)*−Ge(2)*	2.3078(16)
Ir(1)−Ge(2)*	2.5287(10)	C−O (avg)	1.15(2)
Ir(1)−Ir(2A)−Ir(1)*	139.66(4)	Ir(2A)−Ir(1)−Ge(1A)	50.88(9)
Ir(1)−Ge(1A)−Ir(2A)	69.61(18)	Ir(2A)*−Ir(1)−Ge(2)	94.84(3)
Ir(2A)−Ir(1)*−Ir(2B)*	52.08(3)	Ge(3)−Ir(1)−Ge(2)*	103.15(4)

[a] Estimated SDs in the least significant figure are given in parentheses.

graphically and were found to bridge the Ir(1)−Ir(4) and Ir(2)−Ir(4) bonds. The bond-lengthening effect usually associated with bridging hydrido ligands was observed as the distances of Ir(1)−Ir(4) and Ir(2)−Ir(4) [2.8895(4) and 2.9744(4) Å, respectively] are significantly longer than that of the Ir(3)−Ir(4) [2.7230(4) Å] bond, which does not contain a bridging hydrido ligand.[13]

The structural analysis of **11** shows that the molecule is centrosymmetric and that the metal atoms Ir(2) and Ge(1) are disordered equally over two sites. The carbonyl ligands bonded to Ir(2) [C(21)−O(21) and C(22)−O(22)], as well as one phenyl ring bonded to Ge(1) [C(37)−C(42)], are also

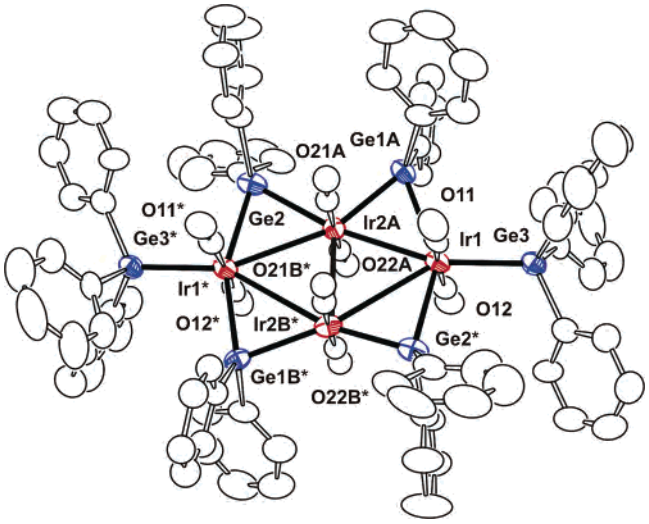

Figure 2. ORTEP diagram of the molecular structure of $Ir_4(CO)_8(GePh_3)_2(\mu\text{-}GePh_2)_4$ (**11**) showing 30% thermal ellipsoid probabilities. For disordered atoms, only one representation is given.

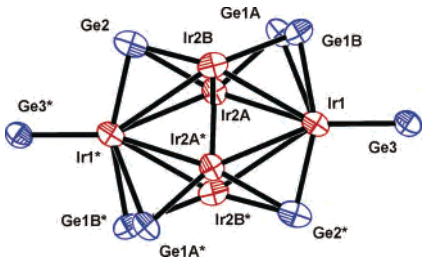

Figure 3. ORTEP diagram of the metal core of **11** showing 40% ellipsoid probabilities. Atoms Ir(2) and Ge(1) are disordered equally over two sites.

disordered over two positions in a 1:1 ratio. An ORTEP diagram of the molecular structure of **11** showing a representation without the disorder is shown in Figure 2. A diagram of the metal core of **11** showing the disordered atoms is shown in Figure 3. Selected intramolecular distances and angles are listed in Table 3. The structure consists of a butterfly arrangement of four iridium atoms. Four $GePh_2$ ligands bridge each of the peripheral Ir−Ir bonds, and two terminal $GePh_3$ ligands are bonded to the two iridium atoms, Ir(1) and Ir(1)*, at the "wingtip" positions. All of the Ir and Ge atoms lie in the same plane, and each iridium atom is bonded to two carbonyl ligands that are oriented perpendicular to this plane. The peripheral Ir−Ir bonds [range 3.3720(11)−2.9070(10) Å] are longer than the central bond of Ir(2A)−Ir(2B)* [2.7690(10) Å]. Compound **11** was also obtained from **10** in 35% yield by reaction with an additional quantity of Ph_3GeH at 97 °C.

The molecular structures of **12** and **13** are shown in Figures 4 and 5, respectively. Selected intramolecular bond distances and angles are listed in Table 4. Both compounds contain only three iridium atoms. Compound **12** consists of a closed Ir_3 triangle with one terminal $GePh_3$, three bridging $GePh_2$, and one triply bridging GePh ligand. The Ir−Ir bond distances [2.8297(4)−2.8785(4) Å] are much longer than those found in $Ir_4(CO)_{12}$ [2.696(1) Å].[14] Triply bridging GePh ligands are very rare, but two were, in fact, observed together

(13) Teller, R. G.; Bau, R. *Struct. Bonding (Berlin)* **1981**, *41*, 1.

(14) Churchill, M. R.; Hutchinson, J. P. *Inorg. Chem.* **1978**, *17*, 3528.

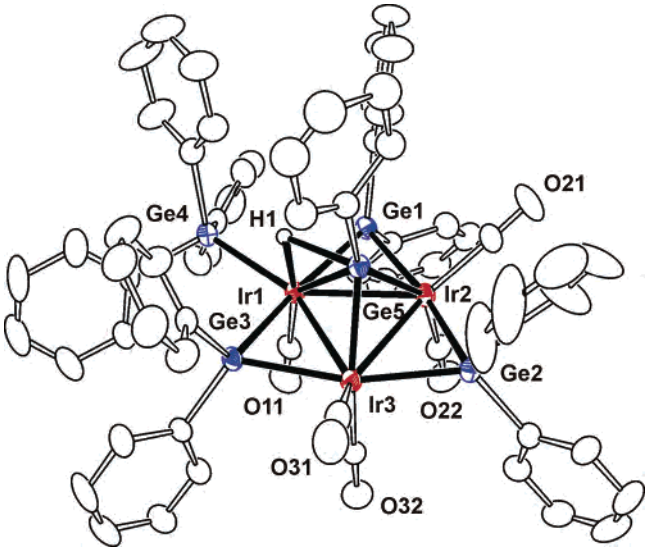

Figure 4. ORTEP diagram of the molecular structure of $Ir_3(CO)_5(\mu\text{-H})(GePh_3)(\mu\text{-}GePh_2)_3(\mu_3\text{-GePh})$ (**12**) showing 30% thermal ellipsoid probabilities.

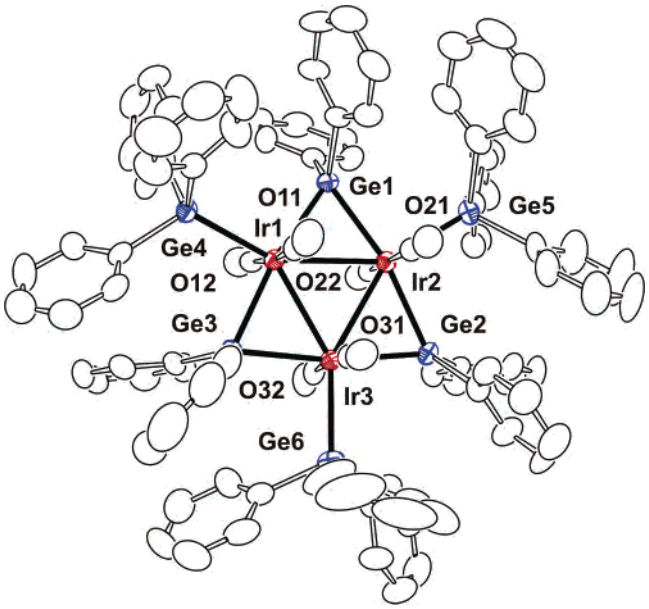

Figure 5. ORTEP diagram of the molecular structure of $Ir_3(CO)_6(GePh_3)_3(\mu\text{-}GePh_2)_3$ (**13**) showing 30% thermal ellipsoid probabilities.

in the compound $Ru_5(CO)_{10}(\mu\text{-}GePh_2)_2(\mu_3\text{-GePh})_2(\mu_3\text{-H})(\mu_4\text{-CH})$ that was obtained from the reaction of **6** with hydrogen.[7] Compound **12** also contains a single hydrido ligand that was located crystallographically and found to bridge the Ir(1)−Ge(5) bond. As expected, the Ir(1)−Ge(5) bond, 2.6258(3) Å, is significantly longer than the unbridged Ir(2)−Ge(5) and Ir(3)−Ge(5) bonds, 2.4102(8) and 2.4139(8) Å, respectively. Although there are some examples of hydrido ligands bridging transition metal−tin bonds,[15] this is to our knowledge the first example of a hydrido ligand bridging a transition metal−germanium bond. Compound **12** was also

Table 4. Selected Intramolecular Distances and Angles for Compounds **12** and **13**[a]

12			
Ir(1)−Ir(2)	2.8457(4)	Ir(2)−Ge(1)	2.5368(8)
Ir(1)−Ir(3)	2.8785(4)	Ir(2)−Ge(2)	2.4823(8)
Ir(2)−Ir(3)	2.8297(4)	Ir(2)−Ge(5)	2.4102(8)
Ir(1)−Ge(1)	2.4798(8)	Ir(3)−Ge(2)	2.5046(8)
Ir(1)−Ge(3)	2.4698(7)	Ir(3)−Ge(3)	2.5495(8)
Ir(1)−Ge(4)	2.4850(8)	Ir(3)−Ge(5)	2.4139(8)
Ir(1)−Ge(5)	2.6253(8)	C−O (avg)	1.13(2)
Ge(1)−Ir(1)−Ge(4)	91.55(3)	Ge(2)−Ir(2)−Ir(3)	55.803(19)
Ge(1)−Ir(1)−Ge(5)	88.34(2)	Ge(3)−Ir(1)−Ge(1)	170.18(3)
Ge(1)−Ir(1)−Ir(3)	115.62(2)	Ge(4)−Ir(1)−Ir(3)	151.48(2)
13			
Ir(1)−Ir(2)	2.9344(4)	Ir(2)−Ge(2)	2.5261(7)
Ir(1)−Ir(3)	2.8971(4)	Ir(2)−Ge(5)	2.5959(7)
Ir(2)−Ir(3)	2.9135(4)	Ir(3)−Ge(2)	2.5559(7)
Ir(1)−Ge(1)	2.5182(7)	Ir(3)−Ge(3)	2.5400(7)
Ir(1)−Ge(3)	2.5653(7)	Ir(3)−Ge(6)	2.5534(8)
Ir(1)−Ge(4)	2.5754(7)	C−O (avg)	1.13(2)
Ir(2)−Ge(1)	2.5455(7)		
Ge(1)−Ir(2)−Ge(5)	100.55(2)	Ge(3)−Ir(1)−Ir(3)	55.016(17)
Ge(2)−Ir(2)−Ge(1)	164.09(2)	Ge(4)−Ir(1)−Ir(2)	149.42(2)
Ge(3)−Ir(1)−Ir(2)	114.828(18)	Ge(5)−Ir(2)−Ir(1)	152.91(2)

[a] Estimated SDs in the least significant figure are given in parentheses.

obtained in 41% yield by reaction of **11** with an additional quantity of Ph_3GeH at 125 °C.

The structure of **13** consists of an Ir_3 triangle with three bridging $GePh_2$ and three terminal $GePh_3$ ligands. It is isomorphous and isostructural with the related tin-containing compounds **7** and **8** that we recently reported.[6] As with compound **11**, all nine metal atoms are coplanar, and each carbonyl ligand, two on each metal atom, lies perpendicular to this plane. The Ir−Ir bond distances in **13** [2.8971(4)−2.9344(4) Å] are similar to those found in the tin homologue **8** [2.9038(11)−2.9323(11) Å]. Molecular orbital calculations were previously preformed on **7** and indicated that the long Rh−Rh bond distances were the result of strong Rh−Sn bonding and weak Rh−Rh interactions.[6] A similar effect is observed here for compounds **10** and **12**, and the unusual length of Ir−Ir bonds is attributed to bonding modifications due to the presence of the edge-bridging germanium ligands.

An ORTEP diagram of the molecular structure of **14** is shown in Figure 6, and selected intramolecular distances and angles are listed in Table 5. Compound **14** consists of an Ir_4 square with four bridging $GePh_2$ and two quadruply bridging GePh ligands. Examples of GeR groups bridging four transition metal atoms are known and include $Co_4(CO)_{11}(\mu_4\text{-GeMe})_2$[16] and $Ni_9(CO)_8(\mu_4\text{-GeEt})_6$.[17] In addition, four hydrido ligands were located and structurally refined. One hydrido ligand is terminally coordinated to each iridium atom, and all are oriented on the same side of the Ir_4 square plane. Four terminal carbonyl ligands are positioned on the opposite side of the Ir_4 plane, with one on each iridium atom. The ^1H NMR spectrum in solution exhibits a single resonance at −12.21 ppm, which is consistent with the structure

(15) (a) Khaleel, A.; Klabunde, K. J.; Johnson, A. *J. Organomet. Chem.* **1999**, *572*, 11. (b) Schubert, U.; Gilbert, S.; Mock, S. *Chem. Ber.* **1992**, *125*, 835. (c) Cardin, C. J.; Cardin, D. J.; Parge, H. E.; Power, J. M. *Chem. Commun.* **1984**, 609.

(16) Foster, S. P.; Mackay, K. M.; Nicholson, B. K. *Chem. Commun.* **1982**, 1156.

(17) Zebrowski, J. P.; Hayashi, R. K.; Bjarnason, A.; Dahl, L. F. *J. Am. Chem. Soc.* **1992**, *114*, 3121.

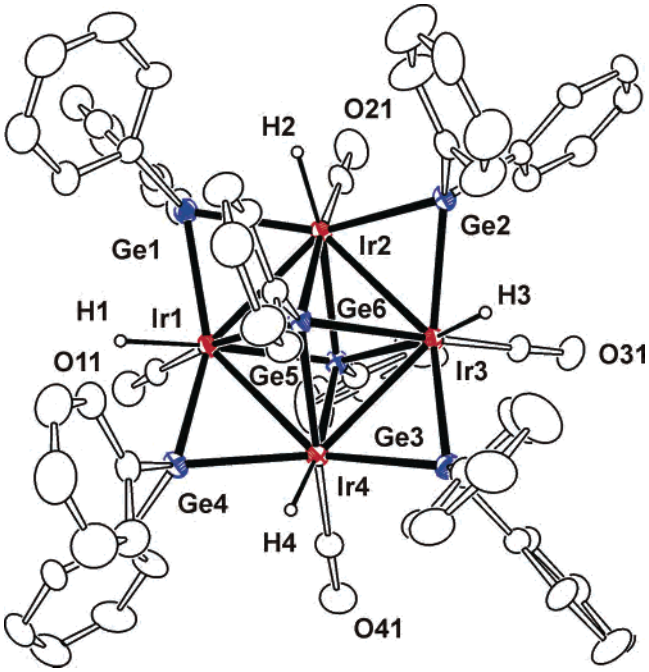

Figure 6. ORTEP diagram of the molecular structure of $Ir_4H_4(CO)_4(\mu\text{-}GePh_2)_4(\mu_4\text{-}GePh)_2$ (**14**) showing 30% thermal ellipsoid probabilities.

Table 5. Selected Intramolecular Distances and Angles for Compound **14**[a]

	14		
Ir(1)−Ir(2)	2.8608(3)	Ir(2)−Ge(4)	2.4535(7)
Ir(1)−Ir(4)	2.8619(3)	Ir(3)−Ge(1)	2.5386(7)
Ir(2)−Ir(3)	2.8567(3)	Ir(3)−Ge(2)	2.5755(7)
Ir(3)−Ir(4)	2.8692(3)	Ir(3)−Ge(4)	2.4482(7)
Ir(1)−Ge(1)	2.5395(7)	Ir(3)−Ge(5)	2.4485(7)
Ir(1)−Ge(2)	2.5787(6)	Ir(4)−Ge(1)	2.5617(7)
Ir(1)−Ge(3)	2.4586(7)	Ir(4)−Ge(2)	2.5636(7)
Ir(1)−Ge(6)	2.4552(7)	Ir(4)−Ge(5)	2.4724(7)
Ir(2)−Ge(1)	2.5564(7)	Ir(4)−Ge(6)	2.4511(7)
Ir(2)−Ge(2)	2.5616(7)	C−O (avg)	1.12(2)
Ir(2)−Ge(3)	2.4459(7)		
Ir(1)−Ir(2)−Ir(3)	90.026(9)	Ir(2)−Ge(1)−Ir(4)	104.66(2)
Ir(1)−Ge(1)−Ir(2)	68.305(18)	Ir(2)−Ge(2)−Ir(4)	104.45(2)
Ir(1)−Ge(1)−Ir(3)	105.56(2)	Ir(2)−Ge(4)−Ir(3)	71.296(19)
Ir(1)−Ge(2)−Ir(2)	67.635(16)	Ir(3)−Ge(5)−Ir(4)	71.330(19)
Ir(1)−Ge(3)−Ir(2)	71.367(19)	Ge(3)−Ir(1)−Ir(2)	54.110(16)
Ir(1)−Ge(6)−Ir(4)	71.367(19)	Ge(3)−Ir(1)−Ir(4)	139.110(18)

[a] Estimated SDs in the least significant figure are given in parentheses.

observed in the solid state. The Ir−Ir bond distances, 2.8567(3)−2.8692(3) Å, are longer than those in $Ir_4(CO)_{12}$. This may be due to the presence of the bridging germyl ligands. Interestingly, compound **14** was also obtained in 39% yield from the reaction of **11** with H_2 at 151 °C. A summary for the interrelationships of compounds **10**, **11**, **12**, and **14** is shown in Scheme 2. In the reaction of $Ir_4(CO)_{12}$ with Ph_3GeH at 97 °C, **10** is presumably formed first and then converted to **11** during the course of the reaction. At 125 °C, compound **11** is then converted to **12** by the loss of one iridium-containing group. Compound **11** reacts with hydrogen at 151 °C to form **14**. Compound **13** was obtained in very low yield from the reaction of $Ir_4(CO)_{12}$ with Ph_3GeH at 125 and 151 °C and could not be obtained from **10**, **11**, or **12**. The electron counting for compounds **10**−**13** is relatively straightforward, and all iridium atoms have the

Scheme 2

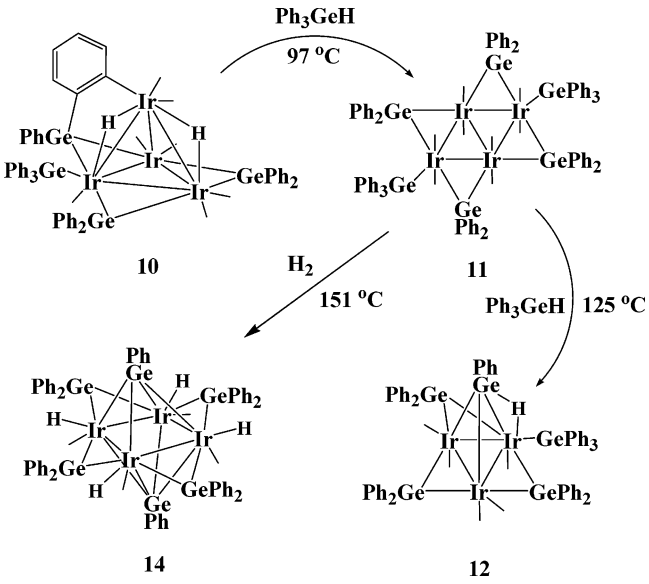

Scheme 3

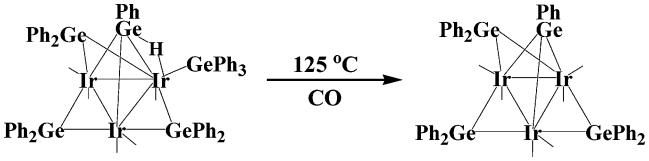

usual 18-electron configuration. However, the total valence electron count for **14** is 62, which is two electrons less than the expected 64 for a square arrangement of four metal atoms. The two μ_4-GePh ligands were each counted as a 3-electron donor to the cluster.

Compound **12** reacts with CO at 125 °C to give the new triiridium cluster complex $Ir_3(CO)_6(GePh_2)_3(\mu_3\text{-}GePh)$ (**15**) in 93% yield. See Scheme 3. An ORTEP diagram of **15** is given in Figure 7. Selected intramolecular bond distances

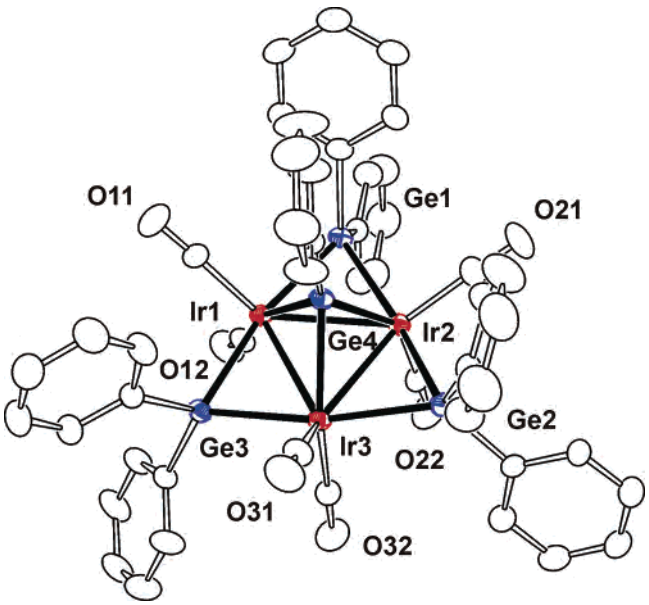

Figure 7. ORTEP diagram of the molecular structure of $Ir_3(CO)_6(\mu\text{-}GePh_2)_3(\mu_3\text{-}GePh)$ (**15**) showing 30% thermal ellipsoid probabilities.

Table 6. Selected Intramolecular Distances and Angles for Compound **15**[a]

15			
Ir(1)−Ir(2)	2.8624(3)	Ir(2)−Ge(2)	2.4920(5)
Ir(1)−Ir(3)	2.8252(3)	Ir(2)−Ge(4)	2.4561(5)
Ir(2)−Ir(3)	2.9034(3)	Ir(3)−Ge(2)	2.4956(5)
Ir(1)−Ge(1)	2.4973(5)	Ir(3)−Ge(3)	2.4851(5)
Ir(1)−Ge(3)	2.4969(5)	Ir(3)−Ge(4)	2.4584(5)
Ir(1)−Ge(4)	2.4365(5)	C−O (avg)	1.13(1)
Ir(2)−Ge(1)	2.4934(5)		
Ir(1)−Ir(2)−Ir(3)	58.676(6)	Ir(2)−Ir(1)−Ir(3)	61.387(7)
Ir(1)−Ir(3)−Ir(2)	59.936(6)	Ir(2)−Ir(1)−Ge(1)	54.940(11)
Ir(1)−Ir(2)−Ge(1)	55.067(12)	Ir(2)−Ge(1)−Ir(1)	69.994(13)
Ir(1)−Ir(2)−Ge(2)	112.730(13)	Ir(2)−Ge(2)−Ir(3)	71.200(14)
Ir(1)−Ge(4)−Ir(2)	71.610(13)	Ir(2)−Ge(4)−Ir(3)	72.425(14)
Ir(1)−Ge(4)−Ir(3)	70.502(13)	Ir(3)−Ir(1)−Ge(1)	116.177(12)

[a] Estimated SDs in the least significant figure are given in parentheses.

and angles for **15** are listed in Table 6. The structure of **15** is similar to that of **12** in that they both contain Ir_3 triangles with three bridging $GePh_2$ ligands and one triply bridging GePh ligand. Compound **15** is formed from **12** by the addition of a single carbonyl ligand and the loss of the hydrido ligand and the terminal $GePh_3$ ligand, but the ultimate fate of these two ligands was not ascertained. The total valence electron count of **14** is 48, which is typical for an electron-precise triangular arrangement of three iridium atoms.

Herein we have described the synthesis and reactivity of the largest iridium−germanium cluster complexes reported to date. Compounds **10**−**14** were synthesized by the reaction of $Ir_4(CO)_{12}$ with Ph_3GeH at various temperatures. An additional complex, **15**, was obtained by the reaction of **12** with CO. This work has further demonstrated the ability of metal clusters to engage in multiple additions of germanium-containing ligands to metal−carbonyl clusters. These and related cluster complexes containing Group 14 elements could be used as precursors to a range of new bimetallic nanoparticle catalysts.

Acknowledgment. This research was supported by the Office of Basic Energy Sciences of the U. S. Department of Energy under Grant No. DE-FG02-00ER14980.

Supporting Information Available: Tables for the structural analyses of **10**−**15**; crystallographic data in CIF format. This material is available free of charge via the Internet at http://pubs.acs.org.

IC0485108